Demonstration of an Optical Quantum Controlled-NOT Gate without Path Interference

Ryo Okamoto,[1] Holger F. Hofmann,[2] Shigeki Takeuchi,[1] and Keiji Sasaki[1]

[1]*Research Institute for Electronic Science, Hokkaido University, Sapporo 060-0812, Japan*
[2]*Graduate School of Advanced Sciences of Matter, Hiroshima University, Hiroshima 739-8530, Japan*
(Received 30 June 2005; published 18 November 2005)

We report the first experimental demonstration of an optical quantum controlled-NOT gate without any path interference, where the two interacting path interferometers of the original proposals [Phys. Rev. A **66**, 024308 (2002); **65**, 062324 (2002)] have been replaced by three partially polarizing beam splitters with suitable polarization dependent transmittances and reflectances. The performance of the device is evaluated using a recently proposed method [Phys. Rev. Lett. **94**, 160504 (2005)], by which the quantum process fidelity and the entanglement capability can be estimated from the 32 measurement results of two classical truth tables, significantly less than the 256 measurement results required for full quantum tomography.

Quantum computing promises to solve problems such as factoring large integers [1] and searching over a large database [2] efficiently. One of the greatest challenges is to implement the basic elements of quantum computation in a reliable physical system and to evaluate the performance of the operation in a sufficient manner. In one of the earliest proposals for implementing quantum computation [3], each qubit was encoded in a single photon existing in two optical modes. The main advantage of the photonic implementation of qubits is the robustness against decoherence and the availability of one-qubit operations. However, the difficulty of realizing the nonlinear interactions between photons that are needed for the implementation of two-qubit operations has been a major obstacle. In recent work, Knill, Laflamme, and Milburn [4] have shown that this obstacle can be overcome by using linear optics, single photon sources, and photon number detectors. By now, various controlled-NOT (CNOT) gates for photonic qubits using linear optics have been proposed [5–10] and demonstrated [11–16].

In particular, it has been shown in Refs. [7,8] that a "compact" CNOT gate can be realized by interaction at a single beam splitter and postselection of the output. Since this gate requires no ancillary photon inputs or additional detectors, it should be especially useful for experimental realizations of optical quantum circuits [17]. However, there have been two crucial difficulties. In the original scheme [7,8], the polarization sensitivity of the operation was achieved by separating the paths of the orthogonal polarizations, essentially creating two interacting two-path interferometers. Therefore, the initial experimental realizations based the original proposal [14,15] are very sensitive to the noisy environment (thermal drifts and vibrations), making it necessary to control and to stabilize nanometer order path-length differences. In addition to these problems, perfect mode matching is required in each output of the interferometer. Thus, it is very difficult to construct quantum circuits using devices based on those experimental setups. Another difficulty is the evaluation of experi-

mental errors in multiqubit gates. In order to obtain the most complete evaluation of gate performance possible, quantum process tomography has been used in the previous experiment [15]. However, 256 different measurement setups are required to evaluate only one CNOT device. When we have to evaluate even more complicated quantum devices realized by a combination of gates, the number of measurements required for tomography rapidly increases as the number of input and output qubits increases.

In this Letter, we present an experimental realization of the compact optical CNOT gate [7,8] without any path interference. We show that the CNOT gate can be implemented using three partially polarizing beam splitters (PPBSs) with suitable polarization dependent transmittances and reflectances, where the essential interaction is realized by a single intrinsic PPBS, while the other two supplemental PPBSs act as local polarization compensators. The gate operation can then be obtained directly from the polarization dependence of the reflectances of the PPBSs, removing the need for interference between different paths for orthogonal polarizations. We have evaluated the device operation using a recently proposed method [18], by which we can determine the lower and upper bounds of the process fidelity from measurements of only 32 input-output combinations. We can thus characterize the gate operation with $1/8$ the number of input-output measurements required for complete quantum process tomography. We hope that these results will open a door to the realization of more complex quantum circuits for quantum computing.

Figure 1(a) shows the previously proposed optical circuit for the CNOT gate [7,8]. The beam splitter sitting in the center of the circuit is the essential one which realizes the quantum phase gate operation by flipping the phase of the state $|H; H\rangle$, where both photons are horizontally polarized, to $-|H; H\rangle$ due to two-photon interference. Since this operation attenuates the amplitudes of horizontally polarized components by a factor of $1/\sqrt{3}$, the other two beam splitters with reflectivity $1/3$ are inserted in each of the
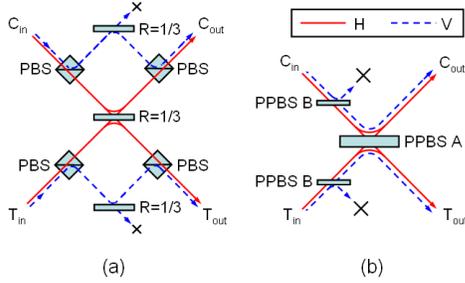
FIG. 1 (color online). Schematics of the compact CNOT gate.
(a) The optical circuit in the original proposals [7,8]. Here the
polarizing beam splitters (PBSs) reflect (transmit) photons with
vertical (horizontal) polarization. (b) The optical circuit without
any path interference using partially polarizing beam splitters.
Note that PPBS-Bs can be placed either before or after the
PPBS-A.

interferometer paths in order to also attenuate the ampli-
tudes of vertically polarized components $|V\rangle$, so that the
total amplitude of any two-photon input is uniformly atte-
nuated to $1/3$. If we now define the computational basis of
the gate as $|0_z\rangle_C \equiv |V\rangle_C, |1_z\rangle_C \equiv |H\rangle_C$ for the control qubit
and $|0_z\rangle_T \equiv 1/\sqrt{2}(|V\rangle_T + |H\rangle_T), |1_z\rangle_T \equiv 1/\sqrt{2}(|V\rangle_T - |H\rangle_T)$ for the target qubit, the gate performs the unitary
operation $\hat{U}_{\text{CNOT}}$ of the quantum CNOT on the input qubits.

The difficulty in the original proposal is that we have to
stabilize the two interferometers of the horizontally and
vertically polarized paths by controlling the length of four
optical paths with an accuracy on the order of nanometers
in order to achieve reliable operation of the device. In
addition, the modes in each path have to be aligned pre-
cisely at the output ports of the polarizing beam splitters.
Such difficulties have been crucial obstacles for the future
realization of optical quantum circuits consisting of several
CNOT gates.

Figure 1(b) shows our solution to this problem. We use
one intrinsic PPBS (PPBS-A) and two supplemental PPBSs
(PPBS-B) in the optical circuit. The intrinsic PPBS-A,
which corresponds to the central beam splitter in
Fig. 1(a), implements the quantum phase gate operation
by reflecting vertically polarized light perfectly and reflect-
ing (transmitting) $1/3$ ($2/3$) of horizontally polarized light.
The two supplemental PPBS-Bs are inserted to adjust the
amplitudes of the local horizontal and vertical components
of the photonic qubits by transmitting (reflecting)
$1/3$ ($2/3$) of vertically polarized light and transmitting
horizontally polarized light perfectly. As Fig. 1(b) shows,
the use of PPBSs allows us to reduce the four optical paths
in Fig. 1(a) to only two optical paths, and path interfer-
ometers are no longer required for the implementation of
the compact quantum CNOT gate.

In the following experimental demonstration, we used a
simple polarization compensation instead of the two sup-
plemental PPBS-Bs. The only purpose of the PPBS-Bs is to
reduce the amplitude of the vertical component in the input
to $1/\sqrt{3}$ of the original input value, while leaving the

horizontal component unchanged. Therefore, we can easily
simulate the function of the supplemental PPBS-Bs by
using compensated input states whose vertical component
is reduced to $1/\sqrt{3}$. To simulate a general input state
$|\psi_{\text{effective}}\rangle = c_H|H\rangle + c_V|V\rangle$, we thus use a compensated
input state of $|\psi_{\text{comp.}}\rangle = c_H|H\rangle + (c_V/\sqrt{3})|V\rangle$. For ex-
ample, the input for the target qubit state $|0_z\rangle_T$ becomes
$|0'_z\rangle_T = (\sqrt{3}|H\rangle + |V\rangle)/\sqrt{6}$, which can be easily prepared
just by changing the angle of linear polarization by rotating
the half-wave plate (HWP) in the target input.

The schematic of our experimental setup is shown in
Fig. 2. We used a pair of photons generated through spon-
taneous parametric down-conversion for our input. A beta
barium borate (BBO) crystal cut for the type II twin-beam
condition [19] was pumped by an argon ion laser at a
wavelength of 351.1 nm. The pump beam was focused in
the BBO crystal using a convex lens to increase the photon
flux [20]. Pairs of twin photons are emitted at 702.2 nm
with orthogonal polarizations. Glan-Thompson polarizers
are used to increase the extinction ratio. After removing the
scattered pump light using bandpass filters (IF, center
wavelength 702.2 nm, FWHM 0.3 nm), each of the photons
was guided to polarization maintaining single-mode fibers
(PMFs) via objective lens and then delivered to the CNOT
verification setup. After the collimation lens for the output
of the PMFs, the polarization of photons are controlled by
HWPs. The timing of the two photons injected to the
PPBS-A was controlled using an optical delay. A quarter-
wave plate was inserted to compensate the phase change
between horizontal and vertical polarization in the optical
delay. After the quantum interference which occurs at
PPBS-A, a dielectric mirror specially made to order, the
polarization of output photons was analyzed using HWPs
and PBSs. Finally, those photons are coupled into single-
mode fibers and counted by the single photon counters
(SPCM-AQ-FC, Perkin Elmer).

Our setup permits us to select various linear polariza-
tions for the input and to detect the corresponding linear
polarizations in the output. As has been shown in Ref. [18],
it is possible to characterize the essential quantum proper-
ties of the gate operation by using the computational ZZ
basis given above and the complementary linearly polar-
ized XX basis given by $|0_x\rangle_C \equiv 1/\sqrt{2}(|V\rangle_C + |H\rangle_C)$,
$|1_x\rangle_C \equiv 1/\sqrt{2}(|V\rangle_C - |H\rangle_C)$ for the control qubit and
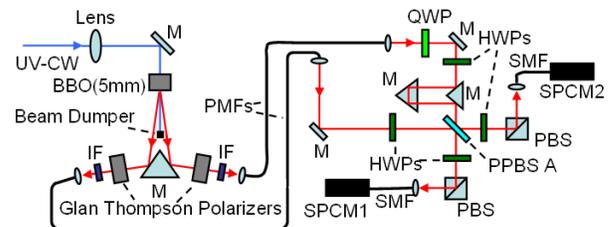

FIG. 2 (color online). Experimental setup for the demonstra-
tion of the CNOT gate without any path interference. M is for
reflecting mirrors.

TABLE I. Measurement results for the input-output probabilities of the CNOT operation in the ZZ basis (a) and the reverse CNOT operation in the XX basis (b).

(a)	$\langle 0_z 0_z |$	$\langle 0_z 1_z |$	$\langle 1_z 0_z |$	$\langle 1_z 1_z |$
$|0_z 0_z\rangle$	0.898	0.031	0.061	0.011
$|0_z 1_z\rangle$	0.021	0.885	0.006	0.088
$|1_z 0_z\rangle$	0.064	0.027	0.099	0.810
$|1_z 1_z\rangle$	0.031	0.096	0.819	0.054
(b)	$\langle 0_x 0_x |$	$\langle 0_x 1_x |$	$\langle 1_x 0_x |$	$\langle 1_x 1_x |$
$|0_x 0_x\rangle$	0.854	0.044	0.063	0.039
$|0_x 1_x\rangle$	0.013	0.099	0.013	0.874
$|1_x 0_x\rangle$	0.050	0.021	0.871	0.058
$|1_x 1_x\rangle$	0.019	0.870	0.040	0.071

$|0_x\rangle_T \equiv |V\rangle_T$, $|1_x\rangle_T \equiv |H\rangle_T$ for the target qubit. The operation of the gate on this input basis also corresponds to a CNOT, with the target qubit acting on the control qubit (reverse CNOT).

The measurement result of the input-output probabilities of our CNOT gate in the ZZ basis and in the XX basis are shown in Table I(a) and (b), respectively. We measured the coincidence counts between two SPCMs by appropriately setting the HWPs for 16 different combinations of input and output states. In order to convert the coincidence rates to probabilities, we normalize them with the sum of coincidence counts obtained for the respective input state. The three dimensional bar graphs of Table I are shown in Fig. 3. The fidelity F_{zz} of the CNOT operation in the ZZ basis, defined as the probability of obtaining the correct output averaged over all four possible inputs, is 0.85. Similarly, the fidelity F_{xx} of the reverse CNOT operation in the XX basis is 0.87.

As discussed in detail in Ref. [18], the two complementary fidelities F_{zz} and F_{xx} define an upper and a lower bound for the quantum process fidelity F_{process} of the gate with

$$F_{zz} + F_{xx} - 1 \leq F_{\text{process}} \leq \min\{F_{zz}, F_{xx}\}. \quad (1)$$

Thus, our experimental results show that the process fidelity of our experimental quantum CNOT gate is
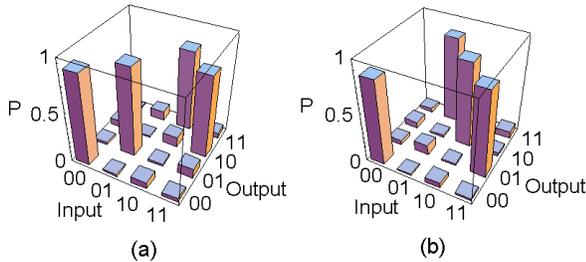

(a)　　　　　　　　　　(b)

FIG. 3 (color online). (a) Bar graph of the experimental results for the CNOT operation in the ZZ basis. (b) Bar graph of the experimental results for the reverse CNOT operation in the XX basis.

$$0.72 \leq F_{\text{process}} \leq 0.85. \quad (2)$$

The lower bound of the process fidelity also defines a lower bound of the entanglement capability of the gate, since the fidelity of entanglement generation is at least equal to the process fidelity. In terms of the concurrence C that the gate can generate from product state inputs, the minimal entanglement capability is, therefore, given by $C \geq 2F_{\text{process}} - 1$ [18]. Since our experimental results show that the minimal process fidelity of the gate is 0.72, the lower bound of the entanglement capability is

$$C \geq 0.44. \quad (3)$$

The experimental results shown in Table I are therefore sufficient to confirm the entanglement capability of our gate.

In order to gain a better understanding of the noise effects in our experimental quantum gate, we can analyze the errors in the classical operations shown in Table I and associate them with quantum errors represented by elements of the process matrix. For this purpose, it is useful to classify the errors according to the bit flip errors in the output of the operations in the ZZ and the XX basis, using 0 for the correct gate operation, C for a flip of the control bit output, T for a flip of the target bit output, and B for a flip of both outputs. It is then possible to expand the process matrix in terms of 16 orthogonal unitary operations $\hat{U}_i$, where the index $i = \{00, C0, T0, B0, 0C, CC, TC, BC, 0T, CT, TT, BT, 0B, CB, TB, BB\}$ defines the pair of error syndromes in the complementary operations in the ZZ and the XX basis, e.g., $\hat{U}_{\text{TC}}$ for a target flip error in the ZZ operation and a control flip error in the XX operation and $\hat{U}_{00} = \hat{U}_{\text{CNOT}}$ for the ideal gate operation. The process matrix describing the noisy gate operation is given by the operator sum representation of the relation between an arbitrary input density matrix $\hat{\rho}_{\text{in}}$ and its output density matrix $\hat{\rho}_{\text{out}}$,

$$\hat{\rho}_{\text{out}} = \sum_{i,j} \chi_{i,j} \hat{U}_i \hat{\rho}_{\text{in}} \hat{U}_j^\dagger. \quad (4)$$

Since each operation $\hat{U}_i$ describes a well defined combination of errors in the ZZ and XX operations, it is now possible to relate the error probabilities observed in Table I to sums over the diagonal elements $\chi_{i,i}$ of the process matrix, as shown in Table II. Since the correlations be-

TABLE II. Relation between experimentally observed errors and process matrix elements. (X = 0, C, T, B).

$\chi_{i,i}$	X0	XC	XT	XB	Sum
0X	$\chi_{00,00}$	$\chi_{0C,0C}$	$\chi_{0T,0T}$	$\chi_{0B,0B}$	0.853
CX	$\chi_{C0,C0}$	$\chi_{CC,CC}$	$\chi_{CT,CT}$	$\chi_{CB,CB}$	0.052
TX	$\chi_{T0,T0}$	$\chi_{TC,TC}$	$\chi_{TT,TT}$	$\chi_{TB,TB}$	0.051
BX	$\chi_{B0,B0}$	$\chi_{BC,BC}$	$\chi_{BT,BT}$	$\chi_{BB,BB}$	0.044
Sum	0.867	0.071	0.034	0.028	1.000

TABLE III. Diagonal elements of the process matrix for (a) the worst case of process fidelity 0.72 and (b) the optimal case of process fidelity 0.85.

(a)	X0	XC	XT	XB	Sum
0X	0.720	0.071	0.034	0.028	0.853
CX	0.052	0.000	0.000	0.000	0.052
TX	0.051	0.000	0.000	0.000	0.051
BX	0.044	0.000	0.000	0.000	0.044
Sum	0.867	0.071	0.034	0.028	1.000
(b)	X0	XC	XT	XB	Sum
0X	0.853	0.000	0.000	0.000	0.853
CX	0.005	0.025	0.012	0.010	0.052
TX	0.005	0.024	0.012	0.010	0.051
BX	0.004	0.022	0.010	0.008	0.044
Sum	0.867	0.071	0.034	0.028	1.000

tween errors in ZZ and errors in XX are unknown, a range of different distributions of diagonal elements $\chi_{i,i}$ is consistent with the experimental data. It is possible to illustrate this range of possibilities by considering the scenarios of lowest and highest process fidelity. The matrix elements of these cases are shown in Table III(a) and (b). In the worst case scenario of a process fidelity of 0.72 shown in Table III(a), each error syndrome is observed only in either the ZZ or the XX basis. Therefore, the errors observed in the ZZ operation can be identified directly with $i =$ C0, T0, B0, and the errors observed in the XX operation can be identified with $i =$ 0C, 0T, 0B. In the optimal case of a process fidelity of 0.85 shown in Table III(b), the diagonal elements of $i =$ C0, T0, B0 for errors only in ZZ are all zero. The remaining errors have been distributed over the other diagonal matrix elements within the constraints given by Table II. Note that the distribution of matrix elements in the optimal case is far more homogeneous than the worst case scenario. The actual process fidelity is, therefore, likely to be closer to the upper limit of 0.85 than to the lower limit of 0.72.

In conclusion, we have demonstrated the first experimental realization of an optical CNOT gate without any path interference by measuring the fidelities of the classical CNOT operations in the computational ZZ basis and in the complementary XX basis. The performance of both operations by the same quantum gate at fidelities of 0.85 and 0.87 indicates that our device has a quantum process fidelity of $0.72 \leq F_{\text{process}} \leq 0.85$ and an entanglement capability of $C \geq 0.44$. Since the gate presented in this Letter requires no path-length adjustments, it should be

ideal for the construction of quantum circuits using multiple gates. The present work may, therefore, provide an important first step towards the realization of optical quantum computation with larger numbers of qubits.

[1] P. W. Shor, SIAM J. Comput. **26**, 1484 (1997).
[2] L. K. Grover, Phys. Rev. Lett. **79**, 325 (1997).
[3] G. J. Milburn, Phys. Rev. Lett. **62**, 2124 (1989).
[4] E. Knill, R. Laflamme, and G. J. Milburn, Nature (London) **409**, 46 (2001).
[5] M. Koashi, T. Yamamoto, and N. Imoto, Phys. Rev. A **63**, 030301(R) (2001).
[6] T. B. Pittman, B. C. Jacobs, and J. D. Franson, Phys. Rev. A **64**, 062311 (2001).
[7] H. F. Hofmann and S. Takeuchi, Phys. Rev. A **66**, 024308 (2002).
[8] T. C. Ralph, N. K. Langford, T. B. Bell, and A. G. White, Phys. Rev. A **65**, 062324 (2002).
[9] T. C. Ralph, A. G. White, W. J. Munro, and G. J. Milburn, Phys. Rev. A **65**, 012314 (2002).
[10] M. A. Nielsen, Phys. Rev. Lett. **93**, 040503 (2004).
[11] T. B. Pittman, B. C. Jacobs, and J. D. Franson, Phys. Rev. Lett. **88**, 257902 (2002).
[12] K. Sanaka, K. Kawahara, and T. Kuga, Phys. Rev. A **66**, 040301(R) (2002).
[13] T. B. Pittman, M. J. Fitch, B. C. Jacobs, and J. D. Franson, Phys. Rev. A **68**, 032316 (2003).
[14] J. L. O'Brien, G. J. Pryde, A. G. White, T. C. Ralph, and D. Branning, Nature (London) **426**, 264 (2003).
[15] J. L. O'Brien, G. J. Pryde, A. Gilchrist, D. F. V. James, N. K. Langford, T. C. Ralph, and A. G. White, Phys. Rev. Lett. **93**, 080502 (2004).
[16] Z. Zhao, A. N. Zhang, Y. A. Chen, H. Zhang, J. F. Du, T. Yang, and J. W. Pan, Phys. Rev. Lett. **94**, 030501 (2005).
[17] It should be noted, however, that the architecture of such circuits will be restricted by the postselection requirement that the two photons are output to different ports [7]. To overcome this problem, it would be useful to develop a new device to filter out the two-photon components in the output.
[18] H. F. Hofmann, Phys. Rev. Lett. **94**, 160504 (2005).
[19] S. Takeuchi, Opt. Lett. **26**, 843 (2001).
[20] C. Kurtsiefer, M. Oberparleiter, and H. Weinfurter, Phys. Rev. A **64**, 023802 (2001).